

# Protonation effect on the nonlinear absorption, nonlinear refraction and optical limiting properties of tetraphenylporphyrin\*

ZHANG Xiao-liang (张校亮)<sup>1\*\*</sup> and CHEN Xiao-hong (陈小红)<sup>2</sup>

1. College of Biomedical Engineering, Taiyuan University of Technology, Taiyuan 030024, China

2. College of Physics and Optoelectronics, Taiyuan University of Technology, Taiyuan 030024, China

(Received 30 September 2018; Revised 15 December 2018)

©Tianjin University of Technology and Springer-Verlag GmbH Germany, part of Springer Nature 2019

Nonlinear optical properties of tetraphenylporphyrin ( $H_2TPP$ ) and protonated tetraphenylporphyrin ( $H_4TPP^{2+}$ ) in toluene were investigated by Z-scan technique using a nanosecond laser with 5 ns pulse at 532 nm. Results show that  $H_4TPP^{2+}$  exhibits weaker nonlinear refraction but enhanced reverse saturable absorption (RSA) and optical limiting performance in comparison with pristine  $H_2TPP$ . Since no nonlinear scattering is observed in  $H_4TPP^{2+}$  under low input fluence, and  $H_4TPP^{2+}$  exhibits weaker nonlinear scattering signals than  $H_2TPP$  under high input fluence, the enhancement of RSA and optical limiting performance can be attributed to the larger ratio of excited state absorption cross-section to that of the ground state of  $H_4TPP^{2+}$ .  $H_4TPP^{2+}$  also exhibits superior optical limiting performance, even better than the benchmark RSA material  $C_{60}$ .

**Document code:** A **Article ID:** 1673-1905(2019)02-0135-4

**DOI** <https://doi.org/10.1007/s11801-019-8157-7>

The development of laser science and technology has motivated an extensive research for designs of optical limiting systems for eye and sensor protection. Among widely investigated materials for optical limiting, organic compounds with extended  $\pi$ -conjugated systems have exhibited strong optical limiting properties due to reverse saturable absorption (RSA), such as phthalocyanines and porphyrins<sup>[1-3]</sup>. In the past decades, people have paid much attention on the modification of porphyrin structures to get a larger ratio of excited state absorption cross-section to that of ground, which usually lead to enhanced RSA and optical limiting properties<sup>[1]</sup>. Compared with various complicated modification approaches for porphyrin, the core of porphyrin can be modified simply by adding acid into the solution, meanwhile, the photophysics and RSA properties of porphyrins are also changed<sup>[4-8]</sup>.

Free base tetraphenylporphyrin ( $H_2TPP$ ) is a common porphyrin which has been used as benchmark for various functional porphyrin<sup>[9]</sup>. Blau et al<sup>[10]</sup> reported that  $H_2TPP$  can be protonated in chloroform during sonication, Liu et al<sup>[7]</sup> reported the nonlinear absorption of  $H_2TPP$  and protonated  $H_2TPP$  ( $H_4TPP^{2+}$ ) in chloroform, however, the reports about the RSA, optical limiting properties of  $H_2TPP$  and  $H_4TPP^{2+}$  in other solvents, such as toluene, were few. What's more, most reports on porphyrins were

concentrated on studies of RSA, but their nonlinear refraction properties are seldom reported so far.

In this paper, we study and compare the nonlinear refraction, nonlinear absorption, optical limiting properties of  $H_2TPP$  and  $H_4TPP^{2+}$  in toluene. Results show that  $H_2TPP$  in toluene can be protonated by adding acid into the solution, while  $H_2TPP$  cannot be protonated in N,N-dimethylformamide (DMF). The  $H_4TPP^{2+}$  in toluene shows decreased nonlinear refraction response but enhanced RSA properties due to the larger ratio of excited state absorption cross-section to that of the ground state of  $H_4TPP^{2+}$ . Although  $H_4TPP^{2+}$  shows the weakest nonlinear scattering signals, it exhibits the strongest optical limiting performance compared with  $H_2TPP$  in toluene,  $H_2TPP$  in DMF and  $C_{60}$  in toluene, due to the enhanced RSA properties.

$H_2TPP$  was bought from Sigma-Aldrich Co., LLC.  $H_2TPP$  was prepared with the concentration of  $2 \times 10^{-4}$  mol/L in toluene.  $H_4TPP^{2+}$  was prepared by adding excess amounts of trifluoroacetic acid into  $H_2TPP$  solutions. In  $H_4TPP^{2+}$ , two more protons were added to the central nitrogens of the porphyrin macrocycle, and this process is reversible.

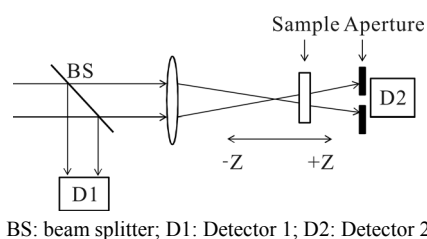
The Z-scan method was utilized to determine simultaneously the magnitude and sign of nonlinear refraction and nonlinear absorption<sup>[11,12]</sup>. The Z-scan experiments

\* This work has been supported by the National Natural Science Foundation of China (Nos.11504259 and 61775157), the Program for the Outstanding Innovative Teams of Higher Learning Institutions of Shanxi, the Scientific and Technological Innovation Programs of Higher Education Institutions in Shanxi (No.2015123), the Natural Science Foundation of Shanxi Province (No.201801D221194), and the Shanxi Special Programs for Platforms and Talents (No.201605D211033).

\*\* E-mail: zhangxiaoliang@tyut.edu.cn

were performed by 5 ns pulsed laser with a 10 Hz repetition rate at 532 nm, generated from a frequency doubled Q-switched Nd:YAG laser (Continuum Surelite-II). A TEM00 Gaussian beam was focused to produce a beam waist radius of 23  $\mu\text{m}$ .

Fig.1 shows the closed-aperture Z-scan experimental apparatus. For the open-aperture Z-scan apparatus, the aperture is removed, and a lens is placed behind the sample to ensure all laser transmitted from the sample can be collected by the detector D<sub>2</sub>.



BS: beam splitter; D1: Detector 1; D2: Detector 2

**Fig.1 The closed-aperture Z-scan experimental apparatus**

For Z-scan experiments, all the solutions were poured in a 1 mm quartz cuvette. All samples were poured in a 5 mm quartz cuvette for optical limiting and nonlinear scattering measurements. For the measurements of optical limiting, the single pulse mode was used, the experimental configuration is the same as those in Refs.[13] and [14]. For nonlinear scattering measurements, a small area lens was placed at 38° with respect to the Z axis to collect the scattered signals. All the samples were adjusted to have the same linear transmittance of 75% at 532 nm for optical limiting and nonlinear scattering measurements. No nonlinear response and damage of the quartz cuvette were observed at the fluence used in our experiments.

The absorption spectra shown in Fig.2 present the characteristic bands of porphyrins. The Soret band of H<sub>2</sub>TPP in toluene is located around 419 nm, and four Q bands are around 514 nm, 548 nm, 591 nm and 648 nm, respectively. Compared with H<sub>2</sub>TPP, the Soret band of H<sub>4</sub>TPP<sup>2+</sup> is located around 438 nm, and there is a red shift of 19 nm. Upon protonation of H<sub>2</sub>TPP, the absorption spectrum of H<sub>4</sub>TPP<sup>2+</sup> in the visible region is characterized by two strong Q bands at 601 nm and 652 nm. Since the protonation process is reversible, the deprotonation can be obtained by adding solvent of DMF. As shown in Tab.1, after adding DMF to the H<sub>4</sub>TPP<sup>2+</sup> toluene solution, Soret band of the products shifts back to 418 nm, and four Q bands emerge at around 514 nm, 549 nm, 591 nm and 648 nm, respectively, which are the same to those of H<sub>2</sub>TPP. This indicates that the deprotonation of H<sub>4</sub>TPP<sup>2+</sup> by the addition of DMF. Our further experiments show that H<sub>2</sub>TPP cannot be protonated in DMF. The absorption spectra data of these three samples are summarized in Tab.1.

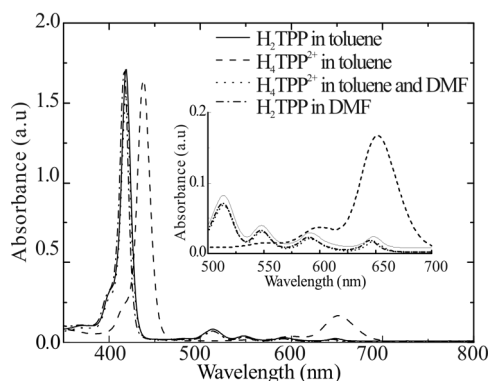


**Fig.2 Absorption spectra of H<sub>2</sub>TPP (in toluene), H<sub>4</sub>TPP<sup>2+</sup> (in toluene), H<sub>2</sub>TPP<sup>2+</sup> (in toluene and followed by adding DMF) and H<sub>2</sub>TPP (in DMF) (Inset shows the Q bands of the samples.)**

**Tab.1 Absorption data of H<sub>2</sub>TPP (in toluene), H<sub>4</sub>TPP<sup>2+</sup> (in toluene), H<sub>2</sub>TPP<sup>2+</sup> (in toluene and followed by adding DMF) and H<sub>2</sub>TPP (in DMF)**

Samples	Soret band,		Q-band, $\lambda_{\text{max}}$ (nm)			
	$\lambda_{\text{max}}$ (nm)					
H <sub>2</sub> TPP	419		514	548	591	648
H <sub>4</sub> TPP <sup>2+</sup>	438		—	—	601	652
*H <sub>4</sub> TPP <sup>2+</sup>	418		514	549	591	648
**H <sub>2</sub> TPP	417		514	548	590	645

“\*” means the solvent is toluene and followed by adding DMF, and “\*\*” means the solvent is DMF.

Fig.3 shows the Z-scan curves of H<sub>2</sub>TPP and H<sub>4</sub>TPP<sup>2+</sup>. As shown in Fig.3(a), the open-aperture curves of H<sub>4</sub>TPP<sup>2+</sup> shows the larger dip, indicating the enhanced RSA by protonation. However, as shown in Fig.3(b), H<sub>4</sub>TPP<sup>2+</sup> exhibits the weaker nonlinear refraction compared with H<sub>2</sub>TPP. Since the dominant mechanism of TPP is RSA arising from excited state absorption, the enhanced nonlinear absorption of H<sub>4</sub>TPP<sup>2+</sup> can be attributed to the change of absorption cross-sections of ground and excited states. In general, the RSA process of organic molecules can be depicted by a five-level mode<sup>[7]</sup>, and the exact calculation of absorption cross-sections of excited states requires rate equation analysis considering all the states in the energy level, but due to unavailability of parameters, such as relaxation times of different states, a simplified three-level model can be used for the estimation of RSA and optical limiting performance<sup>[8,15-17]</sup>. Rate equations of the three-level model can be written as

$$\frac{dN_0}{dt} = -\frac{\sigma_0 I N_0}{\hbar \omega} + \frac{N_{\text{ex}}}{\tau_{\text{ex}}}, \quad (1)$$

$$\frac{dN_{\text{ex}}}{dt} = \frac{\sigma_0 I N_0}{\hbar \omega} - \frac{N_{\text{ex}}}{\tau_{\text{ex}}}, \quad (2)$$

$$\frac{dI}{dz} = -\alpha I = -(\sigma_0 N_0 + \sigma_{\text{eff}}^{\text{ex}} N_{\text{ex}}) I, \quad (3)$$

$$\frac{d\phi}{dz} = k \Delta n = \sigma_r^{\text{ex}} N_{\text{ex}}, \quad (4)$$

where  $N_0$  and  $N_{\text{ex}}$  are the population of the ground state and excited states, respectively,  $\sigma_0$  is the ground state

absorption cross-section, and  $\sigma_{\text{eff}}^{\text{ex}}$  is the effective excited state absorption cross-section (it includes the absorption of the first excited singlet state and the first excited triplet state).  $I$  is input laser intensity,  $\hbar\omega$  is the photon energy,  $\tau_{\text{ex}}$  is the effective decay time of the excited states,  $\alpha$  is the total absorption coefficient,  $\Delta n$  is the change of the refraction index of the sample,  $k$  is the wave vector, and  $\sigma_r^{\text{ex}}$  is the effective refraction cross-section. The ground-state absorption cross-sections  $\sigma_0$  of the samples were calculated from the formula  $\sigma_0 = \alpha_0 / N$ , where  $\alpha_0$  is the linear absorption coefficient, and  $N$  is the number of molecules per cubic centimeter. By theoretically simulating the open-aperture and nonlinear refraction Z-scan experimental data, we can obtain the values of  $\sigma_0$ ,  $\sigma_{\text{eff}}^{\text{ex}}$ ,  $\sigma_r^{\text{ex}}$  and  $\tau_{\text{ex}}$  in the case of 5 ns pulses, and the values are listed in Tab.2.

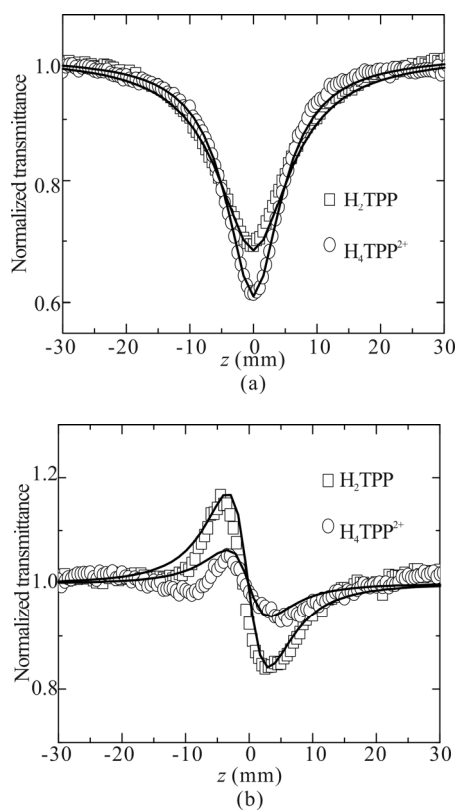


**Fig.3 (a) Open-aperture Z-scan curves and (b) nonlinear refraction curves of H<sub>2</sub>TPP (in toluene), H<sub>4</sub>TPP<sup>2+</sup> (in toluene)**

**Tab.2 Photophysics parameters of the samples at 532 nm**

Samples	$\sigma_0$ ( $\times 10^{-17}$ , cm <sup>2</sup> )	$\sigma_{\text{eff}}^{\text{ex}}$ ( $\times 10^{-17}$ , cm <sup>2</sup> )	$\sigma_r^{\text{ex}}$ ( $\times 10^{-17}$ , cm <sup>2</sup> )	$\tau_{\text{ex}}$ (ns)	$\sigma_{\text{eff}}^{\text{ex}} / \sigma_0$
H <sub>2</sub> TPP in toluene	1.96	6.90	-3.40	4.0	3.52
H <sub>4</sub> TPP <sup>2+</sup> in toluene	0.63	13.5	-2.80	2.5	21.4
H <sub>2</sub> TPP in DMF	0.97	4.20	-	5.0	4.43

It can be seen that H<sub>4</sub>TPP<sup>2+</sup> shows smaller  $\sigma_0$ , larger  $\sigma_{\text{eff}}^{\text{ex}}$  and  $\sigma_{\text{eff}}^{\text{ex}} / \sigma_0$  than those of H<sub>2</sub>TPP, which leads to the enhanced RSA. Fig.3(b) shows the nonlinear refraction Z-scan curves of H<sub>2</sub>TPP and H<sub>4</sub>TPP<sup>2+</sup> obtained by dividing closed-aperture Z-scan data by corresponding open-aperture Z-scan data. It can be seen that H<sub>2</sub>TPP shows negative nonlinear refraction, and  $\sigma_r^{\text{ex}}$  is  $-3.4 \times 10^{-17}$  cm<sup>2</sup> by fitting experimental data. However, H<sub>4</sub>TPP<sup>2+</sup> shows a decreased nonlinear refraction with  $\sigma_r^{\text{ex}}$  of  $-2.8 \times 10^{-17}$  cm<sup>2</sup>, the nonlinear refraction Z-scan curves is not well due to the strong RSA properties for H<sub>4</sub>TPP<sup>2+</sup>, since strong nonlinear absorption always affects nonlinear refraction Z-scan curves<sup>[18]</sup>.

The optical limiting performances of the samples are measured as shown in Fig.4. As shown in Fig.4, H<sub>4</sub>TPP<sup>2+</sup> shows the strongest optical limiting performance, even stronger than C<sub>60</sub>. For example, at the input fluence of 21.5 J/cm<sup>2</sup>, the output fluence values are 1.57 J/cm<sup>2</sup>, 4.06 J/cm<sup>2</sup>, 5.19 J/cm<sup>2</sup> and 7.30 J/cm<sup>2</sup> for H<sub>4</sub>TPP<sup>2+</sup> in toluene, C<sub>60</sub> in toluene, H<sub>2</sub>TPP in DMF and H<sub>2</sub>TPP in toluene, respectively. Nonlinear absorption and nonlinear scattering are two main mechanisms leading to optical limiting effect. To investigate the optical limiting mechanisms in the samples, nonlinear scattering versus input fluence was measured.

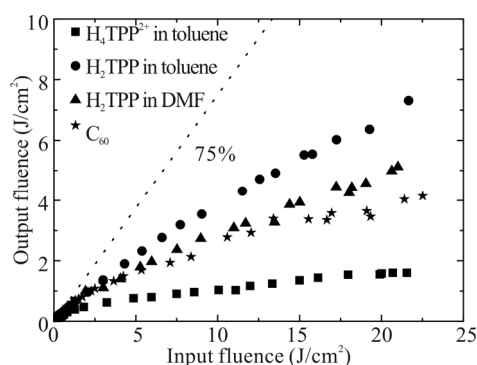


**Fig.4 The optical limiting of H<sub>2</sub>TPP (in toluene), H<sub>4</sub>TPP<sup>2+</sup> (in toluene), H<sub>2</sub>TPP (in DMF) and C<sub>60</sub> (in toluene) with the same linear transmittance of 75%**

As shown in Fig.5, all sample shows the decreasing transmittance as the increase of input fluence, and no obvious nonlinear scattering signals occur for the input fluence lower than 2.0 J/cm<sup>2</sup>. For input fluence higher than 2.0 J/cm<sup>2</sup>, all samples exhibit obvious nonlinear scattering signal. Although H<sub>4</sub>TPP<sup>2+</sup> shows the weakest nonlinear scattering signal, it exhibits the strongest optical limiting performance, indicating the dominant RSA mechanism. Nonlinear refraction arising from excited refraction also contributes to the optical limiting performance of H<sub>4</sub>TPP<sup>2+</sup>, what's more, since H<sub>4</sub>TPP<sup>2+</sup> has a smaller  $\sigma_0$  than that of H<sub>2</sub>TPP for the same linear transmittance, H<sub>4</sub>TPP<sup>2+</sup> has the higher concentration, the higher concentration also leads to large RSA and nonlinear refraction response. So H<sub>4</sub>TPP<sup>2+</sup> shows the best

RSA and optical limiting performance due to the combination of its high concentration and a large value of  $\sigma_{\text{eff}}^{\text{ex}} / \sigma_0$ .

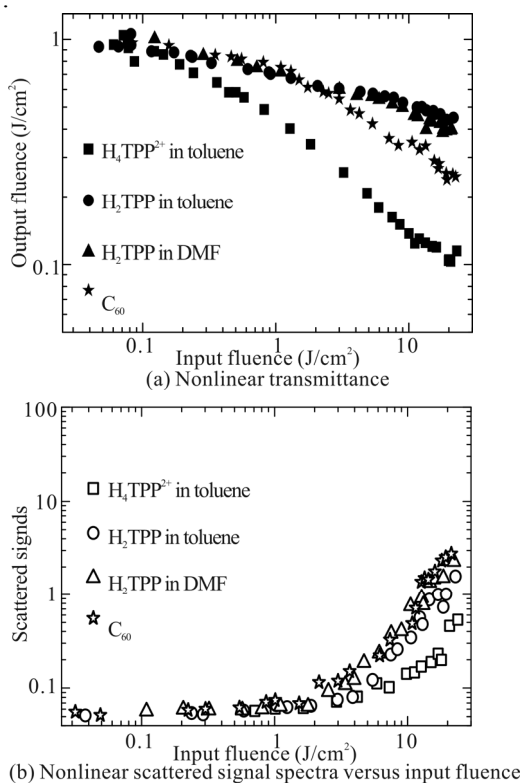


**Fig.5 The optical limiting of H<sub>2</sub>TPP (in toluene), H<sub>4</sub>TPP<sup>2+</sup> (in toluene), H<sub>2</sub>TPP (in DMF) and C<sub>60</sub> (in toluene) with the same linear transmittance of 75%**

In conclusion, nonlinear optics and optical limiting properties of H<sub>2</sub>TPP and H<sub>4</sub>TPP<sup>2+</sup> were investigated. Although H<sub>4</sub>TPP<sup>2+</sup> exhibits weaker nonlinear refraction, it still shows the best RSA, and optical limiting performance due to its large value of  $\sigma_{\text{eff}}^{\text{ex}} / \sigma_0$ , even better than C<sub>60</sub>. The protonation can change the properties of ground and excited states of porphyrins, giving us an approach to conveniently modify and improve the optical limiting performance for porphyrin materials.

**References**

[1] D. Dini, M. J. F. Calvete and M. Hanack, Chemical Reviews **116**, 13043 (2016).

[2] T. M. Pritchett, R. C. Hoffman, A. G. Mott and M. J. Ferry, Applied Optics **56**, B14 (2017).

[3] M. S. S. Bharati, S. Bhattacharya, J. V. Suman Krishna, L. Giribabu and S. Venugopal Rao, Optics and Laser Technology **108**, 418 (2018).

[4] X. Liu, D. Wang, H. Gao, Z. Yang, Y. Xing, H. Cao, W. L. He, H. H. Wang, J. M. Gu and H. Y. Hu, Dyes and Pigments **134**, 155 (2016).

[5] L. H.Z. Cocca, F. Gotardo, L. F. Sciuti, T. V. Acunha, B. A. Iglesias and L. D. Boni, Chemical Physics Letters **708**, 1 (2018).

[6] Y. Wan, Y. X. Xue, N. Sheng, G. H. Rui, C. H. Lv, J. He, B. Gu and Y. P. Cui, Optics and Laser Technology **102**, 47 (2018).

[7] Z. B. Liu, Y. Zhu, Y. Z. Zhu, J. G. Tian and J. Y. Zheng, The Journal of Physical Chemistry B **111**, 14136 (2007).

[8] X. L. Zhang, X. D. Chen, X. C. Li, C. F. Ying, Z. B. Liu and J. G. Tian, Journal of Optics **15**, 055206 (2013).

[9] Blau W J, Byrne H, Dennis W M and Kelly J M, Optics Communication **56**, 25 (1985).

[10] É. M. Ni Mhuircheartaigh, S. Giordani and W. J. Blau, The Journal of Physical Chemistry B **110**, 23136 (2006).

[11] M. Sheik-Bahae, A. A. Said, T. H. Wei, D. J. Hagan and E. W. Van Stryland, IEEE Journal of Quantum Electron **26**, 760 (1990).

[12] Y. C. Zhao, Z.Q. Nie, A. P. Zhai, Y. T. Tian, C. Liu, C. K. Shi and B. H. Jia, Optoelectronics Letters **14**, 21 (2018).

[13] X. L. Zhang, X. Zhao, Z. B. Liu, S. Shi, W. Y. Zhou, J. G. Tian, Y. F. Xu and Y. S. Chen, Journal of Optics **13**, 075202 (2011).

[14] H. Wen, X. L. Zhang, Z. B. Liu, X.Q Yan, X. C. Li and J. G. Tian, Optoelectronics Letters **11**, 161 (2015).

[15] L. F. Sciuti, L. H. Z. Cocca, A. R. L. Caires, P. J. Gonçalves and L. D. Boni, Chemical Physics Letters **706**, 652 (2018).

[16] M. B.M. Krishna, V. P. Kumar, N. Venkatramaiah, R. Venkatesan and D. N. Rao, Applied Physics Letters **98**, 081106 (2011).

[17] P. Gautam, B. Dhokale, V. Shukla, C. P. Singh, K. S. Bindra and R. Misra, Journal of Photochemistry and Photobiology A: Chemistry **239**, 24 (2012).

[18] Z. B. Liu, J. Guo Tian, W. P Zang, W. Y. Zhou, C. P. Zhang and G. Y. Zhang, Chinese Optics Letters **20**, 509 (2003).